AJNR

Interventional MR Imaging: Concepts, Systems, and Applications in Neuroradiology

Jonathan S. Lewin

Interventional MR Imaging: Concepts, Systems, and Applications in Neuroradiology

Jonathan S. Lewin

Recent trends in minimally invasive methods for diagnosis and treatment have created a burgeoning interest in the use of MR imaging for guidance of radiologic and surgical procedures. This review discusses the hardware and software improvements that have made interventional and intraoperative MR imaging a reality. These advances include several different concepts in MR system designs, along with supplemental technological developments in MR pulse sequences, guidance systems, and in-room monitors. This review also describes the use of this technology for minimally invasive diagnostic and therapeutic radiologic procedures, and discusses the application of these techniques for neurosurgical and ear-nose-throat (ENT) intraoperative guidance.

As the practice of neuroradiology has evolved during the past decade, there has been increasing emphasis on intervention, bringing neuroradiologists into a much more prominent role in the care of patients with a growing list of neurologic disorders. Parallel to the development of increasingly sophisticated endovascular and percutaneous radiologic techniques, open neurosurgical procedures have shown a trend toward image-based navigation, endoscopic approaches, and other methods to decrease the invasiveness of more traditional neurosurgery. Radiologic interventional skills and surgical, minimally invasive trends have converged to create a burgeoning interest in the use of MR imaging for guidance of radiologic and surgical procedures.

Historically, the relatively long imaging times and difficulty in patient access resulting from closed-bore superconducting cylindrical system designs have combined to make MR an unlikely guidance technique for either radiologic or surgical procedures. More recently, many of these disadvantages have been overcome with the advent of system hardware and pulse sequence improvements that have allowed the development of rapid imaging on open systems. The purpose of this review is to discuss briefly the hardware and software improvements that have made interventional and intraoperative MR imaging a reality. In addition, the use of this technology for minimally invasive procedures, the technical issues specific to MR image guidance, and the application of MR techniques for intraoperative guidance will also be described.

Imaging System Development

Recent advances in magnet and system design have accelerated progress in MR-guided intervention. Many different MR system configurations have been used to guide percutaneous and surgical procedures. Each of these systems has advantages and disadvantages for interventional and intraoperative imaging, with a constant tradeoff between signal-to-noise, access to the patient, useable field of view, and expense.

Understanding the role of different MR system designs in intervention requires a distinction between image *guidance* and procedural *monitoring*. There are many procedures in which the information provided by MR imaging can be used to monitor a therapeutic intervention. Examples include thermal ablation, in which thermal energy is deposited and the resulting tissue changes are continuously or intermittently observed, or surgical intervention, in which the status of tumor resection or cyst aspiration may be intermittently examined. These forms of interventional MR imaging require much less modification to standard imaging systems because access to the patient is not necessarily required during the monitoring process. Both types of procedures have already been performed on conventional cylindrical superconducting systems (1–3).

The use of MR imaging for interventional guidance includes its use by radiologists during manipulation of needles, electrodes, catheters, or laser fibers, and its application by surgeons for guiding endoscopes, scalpels, or curettes. This form of more active intervention requires a significant departure from conventional diagnostic concepts and traditional imaging systems. The most basic form of this type of guidance can be provided from a retrospective data set through the use of frameless or frame-based stereotactic systems, but increasing emphasis has been on the use of real-time or near-real time guidance for interventional MR imaging procedures.

The factors contributing to high image quality in diagnostic MR include system field strength and the homogeneity and stability of the static and gradient magnetic fields. These factors are most obtainable by decreasing the "openness" of an

imaging system. The optimal design of a magnet with regard to field homogeneity would be a complete sphere, without opening (4). In contrast, the environment best suited to radiologic or surgical intervention is one with maximum access to the patient, allowing complete freedom in interventional approach, and maintaining close proximity of monitoring and therapeutic devices. These attributes are in direct opposition to those facilitating image quality (4). The use of MR imaging for guidance of interventional procedures has required compromise between these opposing forces; this balance has been achieved through a number of different concepts and solutions.

Some of the first interventional procedures under MR image guidance were performed on conventional cylindrical systems, simplifying imaging but significantly compromising the access to the patient that is necessary for performance of the procedure and monitoring of patient discomfort and safety. Biopsy and aspiration procedures have been and can be performed using these cylindrical superconducting systems, but the patient must be withdrawn from the magnet in order to reposition the needle between scans (5). This resulted in relatively long procedure times, and contributed to the lack of widespread use of MR imaging for biopsy and aspiration during the late 1980s. In particular when the lesion in question was visible and accessible for biopsy under CT or sonography, these more conventional methods for procedural guidance were clearly better suited techniques.

These disadvantages were overcome, in part, through the access to the patient provided by permanent or resistive "open" magnet imaging systems (6–9). Unfortunately, the open low-field imaging systems available in the late 1980s often required significant imaging time to obtain sufficient signal-to-noise to allow needle insertion under MR image guidance. Nonetheless, the access to the patient provided by these systems led to an increased number of reports of its use, primarily for biopsy in the head and neck region (10–12).

Since then, many magnet, gradient, and receiver chain-design improvements have led to a number of approaches for interventional imaging. The following is a brief description of the most commonly used current designs for intervention. Each system has benefits and limitations for interventional procedure guidance, as each has chosen a different balance between the spatial constraints necessary for high-quality imaging and the freedom necessary for surgical or radiologic intervention.

Cylindrical Superconducting Systems

From an image-quality viewpoint, cylindrical superconducting systems enjoy many significant advantages relative to static magnetic field strength and homogeneity, and the adoption of this system design as the standard for image quality in the diagnostic arena is not a chance occurrence. The limited patient access for procedural performance, and direct visual observation, is a compromise that still allows certain procedures. The excellent signal-to-noise achieved with these systems is well suited to thermal monitoring during ablation, and has been used during laser and radiofrequency ablation procedures in the brain and in the head and neck (1, 2, 13–16). The investigators in these studies limited the use of MR imaging to the thermal monitoring of the tumor destruction process, and typically inserted the laser fiber or radiofrequency electrode under CT guidance or used a neurosurgical stereotactic approach based on retrospective MR data.

Another approach to the use of cylindrical superconducting systems for interventional monitoring has been the siting of a superconducting system in a surgical environment. With the rapid falloff of the static magnetic field achieved by actively shielded magnet designs, it is possible to site a superconducting system in near proximity to a surgical work space. This design has been adopted for a system constructed by Philips Medical Systems (Eindhoven, The Netherlands) (Fig 1), in which a procedure suite with most of the amenities of a conventional surgical theater has been constructed just outside of the fringe-field of a superconducting short-bore 1.5 tesla (T)

FIG 1.   Superconducting short-bore system. The solution proposed by Phillips, sited in this example at the University of Minnesota, includes a standard short-bore superconducting 1.5 T MR imager adjacent to a surgical work-space that includes C-arm fluoroscopy. A custom table can slide from the surgical work-space into the magnet for intermittent imaging at appropriate times during the surgical intervention. The C-arm fluoroscopic unit can also assist with angiographic procedures. (Photo courtesy of Charles L. Truwit, MD, University of Minnesota)

imaging system. Surgery can be performed in the surgical portion of the suite much as in a conventional operating room. When desired, however, intermittent images can be obtained by sliding the patient into the cylindrical imaging system. The imaging system allows all of the standard capabilities of a high-field system, including functional imaging, with high image quality. Although there are very few compromises to either the surgical or imaging portion of this environment, this configuration does not allow interactive guidance of the intervention, as access to the patient is markedly limited. Direct observation by the anesthesiologist is not possible during scanning, and antisepsis is a challenge because the inside of the cylindrical magnet cannot be easily draped. In the future, the use of this type of system for active procedural guidance may be achieved through the application of robotic systems, but would require significant modification of current surgical or interventional radiologic techniques (Personal Communication, Dr. Charles Truwit, University of Minnesota).

Another recent area of research interest has been the development of MR methods for guidance of angiographic procedures. Although access to the patient's anatomy in the magnet isocenter of a cylindrical magnet is limited, short-bore superconducting systems do allow a degree of access to the patient's groin. Several groups are investigating the use of this type of system for catheter-based intervention, with the radiologist controlling the procedure from the groin near the magnet aperture (17). The Philips system shown in Figure 1 includes a C-arm fluoroscope to facilitate this type of procedure. To date, MR methods for catheter guidance remain rather primitive, and no significant clinical data has yet been published. The use of cylindrical magnets has also been applied outside of neuroradiology, for guidance of stereotactic biopsy for breast lesions (18). This type of stereotactic procedure lends itself well to the breast, but is less applicable to the neuroradiologist's areas of interest.

"Double Donut" Configuration

A novel approach to obtaining access to a patient in a cylindrical system is exemplified in the "double donut" configuration of the Signa SP system (General Electric Medical Systems, Milwaukee, Wis), designed specifically for interventional

FIG 2. "Double donut" design is shown. General Electric Medical Systems Signa SP scanner consists of two very short superconducting cylindrical magnets separated by a 54-cm space to allow physician or nurse access. The space between the two magnet halves allows patient access from the top or sides, typically used with the surgeon and assistant on opposite sides of the patient's head. An optically linked frameless stereotactic tracking system is integrated into the top support piece. The scanner is designed for an operating-room environment, with electrical outlets and anesthesia gases integrated into the magnet covers. This system has a large fringe field, and all surgical instruments and accessory equipment in proximity to the system must be MR-safe or MR-compatible. (Photo courtesy of John Schenck, MD, PhD, and Robert W. Newman, MS, General Electric Medical Systems.)

applications (Fig 2) (19–21). This design has taken the central segment out of a cylindrical system, allowing access to the patient from the sides and top at the isocenter of the imaging system. This product design has been directed toward siting in a surgical environment, and allows enough room in the gaps between the halves (54 cm) for two small- to medium-sized physicians or nurses, one on either side of the patient (4). This system provides a marked improvement in access to the patient relative to a closed-bore cylindrical system. This concept rep-

resents the first system designed and constructed specifically for interventional guidance, and is the only system currently available that allows complete vertical and side access to the patient at the imaging isocenter. This magnet design has been used both to guide and monitor a large number of surgical procedures, in addition to an early published series of biopsies and aspirations (20, 22, 23). Nonetheless, the marked improvement in access to the patient is achieved at the expense of decreased field strength at the imaging isocenter (0.5 T), as compared to the field generated by each individual superconducting half, and compromises magnetic field homogeneity (4). The unobstructed side and vertical access to the patient also complicates the engineering of the radiofrequency coil, requiring a local transmit-receive coil with a somewhat limited field of view.

Biplanar Magnet Designs

Another approach that has found widespread application for diagnostic MR imaging in the burgeoning "open" MR imaging market has been the use of a biplanar magnet design. With these magnets, the patient is positioned between flat magnetic poles, leaving access from a range of side approaches. These systems typically use lower-field permanent or resistive magnets, with field strengths ranging from 0.064 T to 0.3 T, although superconducting mid-field models of this design have also been introduced. The degree of access around the circumference of the biplanar magnet depends upon the number and position of supports separating the two magnetic poles.

A large degree of access around the circumference is afforded by the "C-arm" design, produced by Siemens Medical Systems (Erlangen, Germany) and Picker International (Highland Heights, Ohio). In this design, a single column on one side of the patient supports the upper pole, allowing access from the contralateral side as well as the head- and foot-end of the magnet (Fig 3). Several manufacturers produce biplanar systems with two supporting posts, resulting in slightly more restricted access to the patient. These include systems produced by Fonar Corporation (Melville, NY), Hitachi Medical Corporation of America (Twinsburg, Ohio), and General Electric Medical Systems. There are also designs with four support posts from Toshiba America Medical Systems (San Francisco, Calif) and Fonar Corporation. The biplanar concept has the advantage of a fairly homogeneous static magnetic field, but
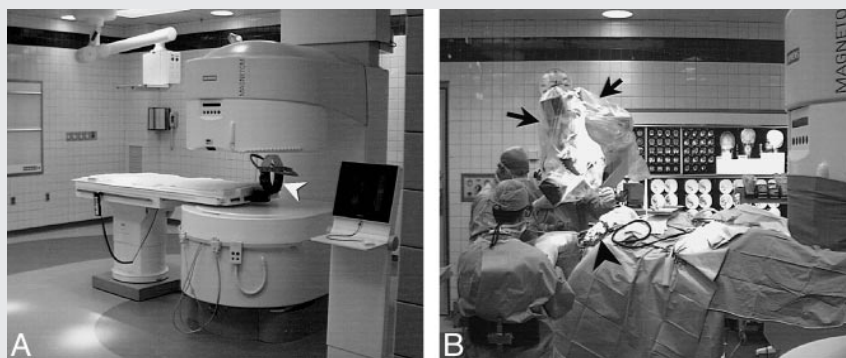

FIG 3. Biplanar system is shown.

A, Siemens Magnetom Open Viva system located in the operating room complex at University Hospitals of Cleveland. With head in imaging position, side access is possible, but the upper magnet pole blocks direct vertical access. Head fixation during surgery is provided with a prototype coil developed by the Heidelberg Neurosurgical Group (*arrowhead*). Concentric markings on the floor signify 20-mT (200-gauss), 0.5-mT (5- gauss), and 0.15-mT (1.5-gauss) field lines. Anesthesia gas columns, telephone, computer connections, and surgical lighting and ventilation meet same requirements as adjacent standard surgical suites.

B, As a variation on the "neighboring work-space" concept, the head end of the table can be smoothly rotated 120° from the magnet bore on a fixed base for surgical procedures, placing the surgical field (*arrowhead*) beyond the 5-gauss line. In this rotated operating position, the table can be tilted or raised to allow standard surgical positioning of the patient, and access for the surgeons and anesthesiologist is identical to a standard surgical suite. Because the surgical field is at less than 5-gauss field strength, standard surgical instruments, a standard Zeiss neurosurgical microscope (*arrows*), as well as standard ultrasonic suction-aspirator, electrocautery, and cortical stimulation equipment can be used. Retractors, curettes, and other equipment used in the magnet bore during image acquisition for monitoring or guidance must be MR-compatible.
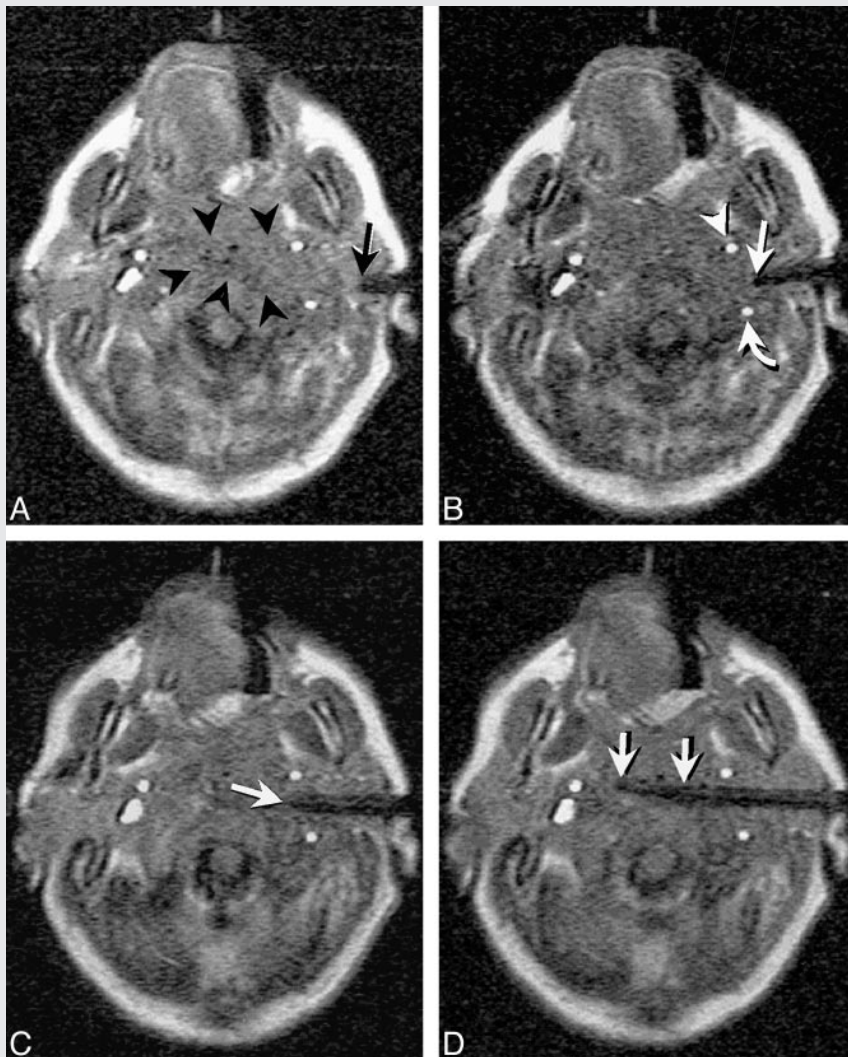
FIG 4. Continuous MR imaging guidance mode. Images from continuous series obtained at 7 seconds/image with Fast Imaging with Steady-state Precession (FISP) sequence (18/7/4/90°, TR/TE/number of signal averages/ flip angle) obtained during guidance of needle insertion in a 68-year-old man with C1–2 vertebral and prevertebral mass. Previous attempt at surgical transoral biopsy had been unsuccessful.

A, An image obtained early during insertion shows needle tip passing through the left parotid space (*arrow*). A poorly defined mass can be seen in the prevertebral space (*arrowheads*).

B, High vascular conspicuity resulting from 2D Fourier transform technique allows ready visualization of flow-related enhancement within the internal carotid (*arrowhead*) and vertebral (*curved arrow*) arteries. The needle tip (*straight arrow*) can be interactively directed to avoid these major vascular structures. The internal jugular vein is only visible during portions of the respiratory cycle. Although visible on the right, the vein was obstructed on the left side of this patient.

C, The needle (*arrow*) is interactively redirected more anteriorly once safely beyond the internal carotid artery (ICA) to allow deployment of the central stylet of the 18-gauge core-cutting needle.

D, After extending the central stylet of the side-notch cutting needle, the notch location is shown as an area of thinning of the distal needle tip (*between arrows*). Histologic findings revealed chronic osteomyelitis and cellulitis and the offending organism was successfully isolated.

is limited to lower field strength than cylindrical superconducting designs. The side access provided by these systems is analogous to that of C-arm fluoroscopy, and is amenable to needle- or catheter-directed procedures. Anterior or posterior interventional approaches, however, require decubitus or oblique positioning of the patient, which may not be possible with large patients owing to the relatively limited space between the poles of the biplane magnet. A true direct vertical approach to the patient is only possible when the patient table is brought outside of the magnet, essentially excluding simultaneous vertical intervention and imaging.

Alternative Magnet Designs

The ultimate design of the interventional MR system of the future is still unclear, given the advantages and above-described limitations. Several alternative concepts are being pursued. One prototype biplanar system has been developed in which the usual horizontal gap between magnet poles has been rotated 90º to allow direct vertical access to the patient, at the expense of side access (4). Other concepts for intervention also have been evaluated, including a head-only superconducting C-arm design (4) and a ceiling-mounted movable magnet (24), although these systems are still in early stages of development. A biplanar design with a very large interpole distance approaching a ''flat bed'' scanner was also recently described by Fonar Corporation, but is still in development. Most likely, different system designs will be advocated for different interventional applications. The choice of interventional system will depend upon each institution's optimal balance between the types of procedures to be performed, required image quality, and financial constraints.

Supplemental Technical Developments

There are several recent technical developments that are common to many of the magnet and system designs discussed above that have facilitated the guidance phase of interventional procedures in a time-efficient manner. First, the construction of higher quality low-noise receiver chains has allowed lower field systems to be constructed, providing relatively high signal-to-noise ratio images, greatly improving image quality when compared to earlier attempts at low-field MR imaging. These systems now provide image quality sufficient for both the monitoring and procedural guidance phases of surgical and minimally invasive procedures. Image acquisition times of 1–3 seconds per image or less provide the necessary temporal resolution.

The second development that has impacted the use of MR methods for procedure guidance has been the modification and development of rapid gradient-echo (GE) pulse sequences for use in interactive guidance during device placement. Rapid GE sequences have been developed to allow a wide range of tissue contrast in a time frame sufficient for device tracking (0.3–7 s per image), even at low field strength, and with the suboptimal coil position sometimes required to access the puncture site (Fig 4) (25–28). Because the area of interest to the interventionalist is often limited to a small portion of the entire image

acquired, a number of strategies have been proposed to decrease further imaging time of these methods. These strategies include alternative reconstruction techniques such as keyhole imaging, singular value decomposition, and wavelet encoding (29–41). The use of these rapid GE techniques for guidance of interventional procedures also benefits from reduced needle artifact at lower fields as compared to 1.5 T, allowing a wider choice of materials for device construction. This advantage also yields high spatial accuracy despite the increased metallic artifact encountered with GE techniques (42, 43).

The third innovation of significant benefit for MR-guided intervention has been the development of an interface between optically linked (three-dimensional) 3D digitizer and the measurement control software of the MR imager. Previously, frameless stereotactic systems had been used primarily for surgical guidance based on historical imaging data sets. The ability to acquire MR images rapidly and interactively in an arbitrary plane determined by a hand-held, sterile probe, or other interventional device, allows rapid planning and confirmation of complex trajectories for rigid instruments. This type of interactive image guidance system was first described as a component of the ''double donut'' system (Fig. 2), and subsequently has been applied for guidance of image acquisition on C-arm systems (Fig 5) (20, 27).

An additional technical factor facilitating near-real-time procedural guidance has been the ability to view images in the magnetic field through the development of in-room high-resolution radiofrequency-shielded monitors (20, 27, 44). In combination with the patient access allowed by open imaging systems, the ability to view images at scanner-side allows the entire procedure to be performed with the operator sitting next to the patient, with no need to remove the operator's hand from the interventional device at any time (Fig 5). This manner of intervention, analogous to an angiographically or sonographically guided procedure, is well suited to the skill set developed by radiologists during more conventional types of image-guided intervention.

MR-Specific Issues for Instrument Guidance and Visualization

Unlike guidance by X-ray-based techniques such as fluoroscopy and CT, there are a number of user-defined imaging parameters and needle trajectory decisions that can markedly alter device visibility and, therefore, accuracy and safety of MR-guided procedures (27, 42). The most important pulse sequence issues affecting visibility of a needle or other thin instrument are the sensitivity of the sequence to magnetic susceptibility effects, and the direction of frequency encoding (42). Optimal imaging during needle insertion also depends upon needle composition, and the angle between the needle shaft and the static magnetic field of the MR imager. As the needle or other thin instrument is positioned parallel to the static magnetic field (vertically for most biplanar magnets and along the long axis of cylindrical or ''double-donut'' systems), artifact at the device tip blooms and obscures the true tip position. On the other hand, the artifact along the shaft of the device diminishes markedly, making it difficult to identify thinner needles or electrodes in the image. The physical basis of these effects is beyond the scope of this review, but has been well described in the literature (27, 42, 43). Safe clinical application of MR-guided techniques requires careful consideration of these factors during procedural planning and execution.

Biopsy and Aspiration

One of the most straightforward interventional applications for a cross-sectional imaging technique is percutaneous biopsy and aspiration. The tissue contrast, spatial resolution, and multiplanar capabilities of MR have obvious benefits for guidance of biopsy and aspiration applications, and this application was the first reported use of MR imaging to guide intervention. As noted above, a number of investigators have described the use of MR imaging for guidance of biopsy and aspiration over the last decade and a half, and much of this early work has been performed for diagnosis of lesions in the head and neck (6, 10–12, 27, 45). The rapid acceptance of MR guidance for head and neck biopsies has occurred, at least in part, because of the striking advantages that MR guidance provides for interventional procedures performed in areas of complex anatomy. The benefits of multiplanar image acquisition were quickly discovered by Lufkin and colleagues, who first reported the advantages derived from going beyond the single imaging plane, usually axial, available in CT-guided procedures (10). The elimination of beam-hardening artifact inherent in CT has also supported the use of MR imaging for guidance of skull base procedures (Fig. 6) (12, 27). Furthermore, the high vascular conspicuity caused by flow-related enhancement effects inherent in two-dimensional (2D) GE imaging is an additional benefit of MR guidance for lesions in regions of complex vascular anatomy (Fig 4).

In our experience, the use of MR imaging for guidance of biopsy and aspiration has been of most advantage in sampling lesions of the suprahyoid neck, including high cervical spinal lesions (Fig 7). The major benefit of MR guidance in this region is its capability to display continuously the internal carotid, vertebral, and major branches of the external carotid artery during the entire needle insertion. Masses at the base of the neck, in particular those encroaching upon the brachial plexus, have also presented an excellent application, exploiting the multiplanar capabilities, tissue contrast, and spatial resolution of MR imaging to allow effective tissue sampling adjacent to the neurovascular structures of the thoracic inlet (Figs 8–9). The capability to guide needle insertion with T2-weighted images has also been helpful for biopsies of laryngeal and pharyngeal submucosal lesions, which are often difficult to define on CT, and may be hidden by normal overlying mucosa on endoscopic examination (Fig 10). T2-weighted techniques can also be used to increase diagnostic tissue yield by allowing sampling of nonnecrotic regions of complex masses.

Depending upon the radiologist's preference, biopsies under MR image guidance can be performed with free-hand methods, needle holders, or using the optically-linked above-described systems (10, 20, 27). Currently, the vast majority of head and neck biopsies at our institution are performed with

FIG 5.   C-arm system for percutaneous intervention is shown. MR suite set up for radiologic intervention has three-camera video sensor array (*curved arrow*) that detects the location and orientation of a hand-held probe (*black arrow*). The system automatically acquires continuous MR images based on the probe position, and automatically updates display of four images on shielded LCD monitor adjacent to the scanner (*arrowhead*). A computer mouse on the LCD console and foot pedals (*not shown*) allow the scanner to be operated by the radiologist throughout the procedure.

free-hand techniques, with optically linked, frameless guidance reserved for particularly complex procedures. Using the free-hand technique, as previously reported (27), most head and neck biopsies can be performed in less than 1 hour of MR table time. For many of these procedures, the rapid frame-rate and high visibility of nearby vessels provided by 2D GE MR techniques allow needle

placement in less time than that required with CT guidance, with less than 8 minutes required per needle pass for both aspiration and core-cutting needle biopsy (27).

Minimally Invasive Percutaneous Therapy

Much of the excitement surrounding MR image-guided procedures has been generated by the tremendous sensitivity of MR imaging for temperature change and depiction of tissue damage. For thermal monitoring, MR imaging provides an unequivocal advantage over the often subtle and indistinct changes noted with CT and sonography. Many of the studies designed for looking at thermal ablation under MR imaging guidance are preliminary, but have shown very encouraging initial results (1, 2, 13–16, 46, 47). The basic premise for using MR imaging to monitor thermal therapy of tumors reflects the capability of MR imaging to show changes in signal directly related to temperature elevation or tissue necrosis, allowing the prediction of lethal tissue damage sites during the heating process (48–52). Although thermal lesion generation without image monitoring is commonly performed in the surgical suite for pain therapy or treatment of movement disorders, the thermal lesion in these cases is limited to a very small size to prevent collateral tissue damage. Thermal lesion volume is often several orders of magnitude larger when therapy is performed for tumor destruction, and the ability to monitor the thermal lesion size and shape becomes essential in order to ensure treatment of the entire target while sparing the sur-
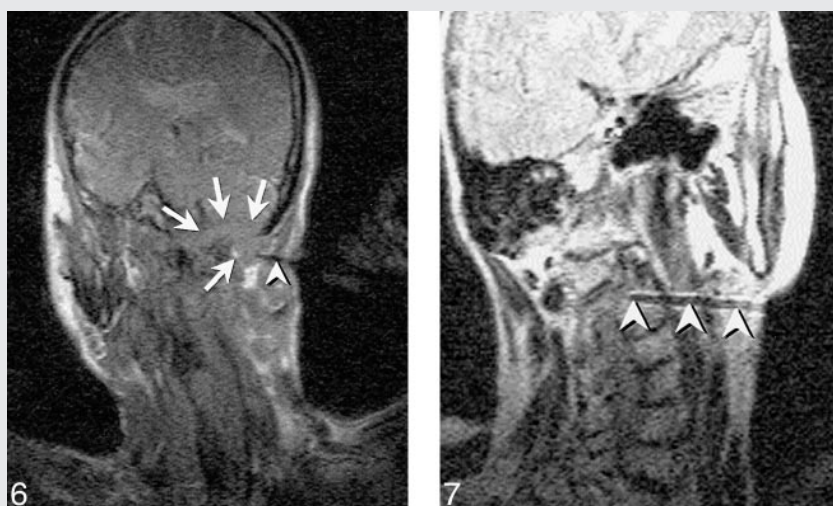

FIG 6.   FISP image shows a skull base mass in a 71-year-old man. A single frame from the continuous series of FISP images (18/7/1/90°) obtained at approximately 1.7 s/image shows needle (*arrowhead*) directed into skull base mass (*arrows*) that destroys the occipital condyle and extends upward into the posterior fossa. This retromastoid approach benefits from the oblique scan planes achieved with MR enabling imaging of the entire craniad and anteriorly angled needle. As typically performed, this scan plane was alternated with the orthogonal view along the path of the needle. Pathologic diagnosis was plasmacytoma.

FIG 7.   MR imaging reveals C2 vertebral body lesion in a 77-year-old woman who reported neck pain. Capability to guide biopsy with oblique imaging plane also allows needle to be angled around internal carotid and vertebral artery for biopsy of high cervical spinal lesions. Turbo spin-echo (SE) T2-weighted image (2000/105/3/17 [TR/TE/NSA/ETL], 51-s scan time) obtained prior to sampling with 18-gauge Menghini-type needle. Frequency encoding must be performed perpendicular to the needle shaft with Turbo SE or SE images to maximize needle visibility. Histologic diagnosis was plasmacytoma, and the patient subsequently developed multiple myeloma.
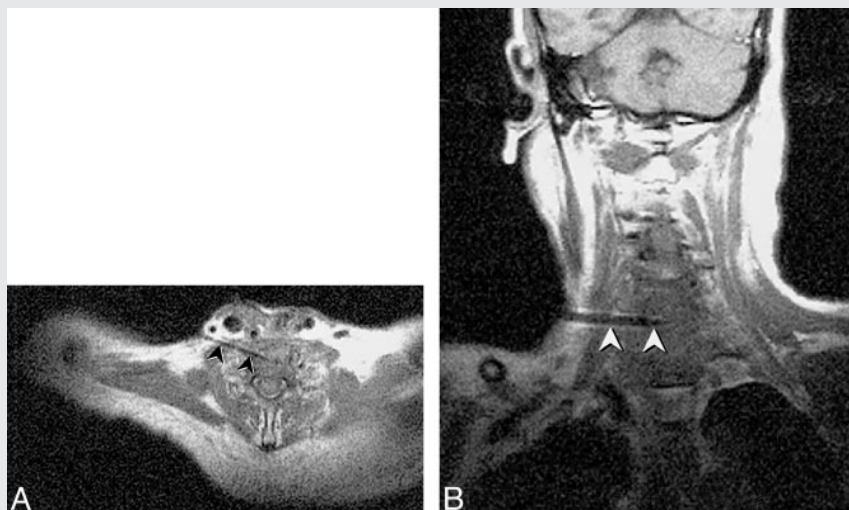
FIG 8. New C6–7 lesion underlying resection site is revealed in a 65-year-old man with history of laryngectomy. Needle placement was performed using FISP guidance (2 s/image), with turbo SE imaging to confirm final placement prior to tissue sampling. Turbo SE T1-weighted axial (*A*) and oblique coronal (*B*) images (680/24/3 [TR/TE/NSA], 106 s scanning time for 3 images) used to confirm 18-gauge Menghini cutting needle placement. The needle (*arrowheads*) can be noted in disk space away from spinal canal or vertebral arteries. Needle was placed through anterior scalene muscle to avoid phrenic nerve and brachial plexus, and was kept anterior to the adjacent vertebral artery. Final diagnosis was fungal osteomyelitis.

rounding normal structures. This is of particular importance for treatment of brain tumors, which are often located near eloquent regions of the cortex (1, 14, 15, 53, 54). The ultimate cost-effectiveness of these procedures remains to be proved, although the remarkably lower cost of MR image-guided tumor ablation, as compared to open surgical excision, provides a strong rationale for the further development of these techniques.

An additional use of MR imaging for percutaneous minimally invasive treatment is in the guidance and monitoring of direct intralesional drug injection, including injection for sclerotherapy of vascular malformations. The same rapid image updates used for interactive needle placement can be used to monitor the injection of sclerosing agents for the treatment of low-flow vascular malformations (55). The multiplanar cross-sectional images obtained with MR imaging allow the injection of alcohol or other sclerosing agents to be monitored during administration, to ensure filling of the entire targeted portion of the malformation and to exclude extravasation or dissipation of the agent through venous egress. MR guidance has been especially helpful in treatment of the insinuating malformations of the head and neck in our experience (Fig 11) (55). The ability to monitor injection, in combination with the tissue contrast capabilities of MR, also lends itself to guidance of other chemical ablation procedures of the head and neck in which precise localization is required.

Intraoperative MR Imaging

A more recent landmark in the evolution of intraprocedural MR imaging has been the development of methods for MR monitoring and guidance during surgical procedures. Neurosurgical interventions have been at the forefront of this development in image-guided surgery, followed by otolaryngological procedures. As MR-guided intervention has extended from percutaneous to more invasive procedures, the degree of complexity in supplemental devices has increased markedly. Much of the inter-

disciplinary effort required for successful implementation of intraoperative MR imaging has been in development and testing of anesthesia equipment, patient monitoring devices, and surgical instruments and accessories (22, 56–59).

Much of the pioneering work in the field of intraoperative MR imaging has been done by Jolesz and associates at Brigham and Women's Hospital in Boston. They were the first to integrate successfully the many components necessary for intraoperative imaging on the 0.5-T General Electric Signa SP system when they performed their first neurosurgical biopsy in June 1995 (22). The idea of constructing neighboring surgical and MR environments with a 0.2-T system was subsequently realized by Tronnier and colleagues in Heidelberg when they completed their first neurosurgical procedure in December 1995 (56). This concept was subsequently modified and applied by several other groups at 0.2 T (57–59). A similar concept was also adopted by the research group at University of Minnesota, who has performed a large series of surgeries using a Philips 1.5-T system for intraoperative monitoring (3). Although these groups, and a number of other investigators with preliminary data not yet published, span a number of different magnet designs, field strengths, and investigational concepts, there are many similarities in the information they have obtained by MR imaging to guide and monitor the surgical procedure.

Considering the complexity of intraoperative MR imaging, it is important to examine the benefits that it may provide over more traditional methods for surgical navigation. Intraoperative MR methods have been advocated to guide instruments to the site of an abnormality, minimize the size of craniotomy necessary for lesion exposure, identify adjacent structures for maximal normal tissue preservation, determine completeness of tumor resection, and provide surveillance for intraoperative complications (22, 56). In addition, intraoperative MR imaging can be used to guide real-time intervention such as neurosurgical biopsy or cyst aspiration dynamically, and verify the accuracy of

FIG 9.   Right supraclavicular fullness is shown in a 52-year-old man who previously underwent left lung resection for carcinoma. The surgeon's physical examination revealed generalized fullness, but no discrete mass.

A, Turbo SE T2-weighted image (2000/105/2 [TR/TE/NSA], 59-s scanning time) reveals focal mass displacing the brachial plexus (*arrow*).

B, Single frame from continuous series of coronal FISP images (18/7/2/90°[TR/TE/NSA/flip angle], 3.5 s/image) shows 18-gauge side-notch cutting needle (*arrowhead*) inserted into the dominant mass.

C, Oblique parasagittal FISP image, orthogonal to and with same parameters as *B,* reveals needle centered within mass (*arrowheads*) with central stylet extended. The continuous imaging sequence allowed the mass to be separated from adjacent vessels as well as from the adjacent portion of the brachial plexus. Pathologic diagnosis from the biopsy was poorly differentiated large-cell carcinoma.
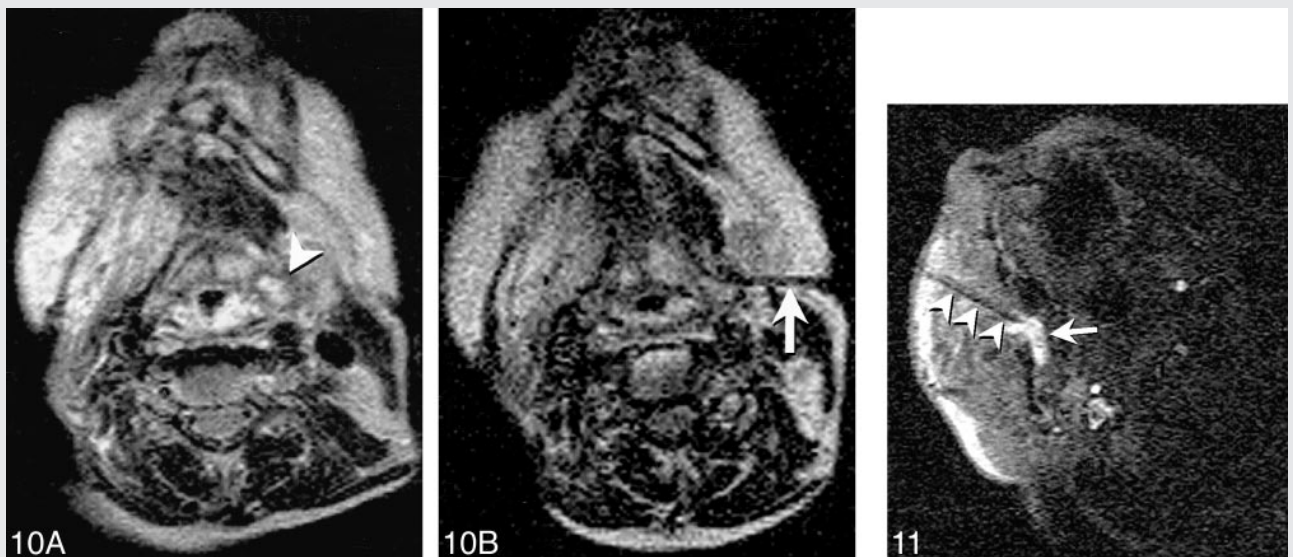

FIG 10.   Imaging of an 80-year-old woman after radiation therapy for squamous cell carcinoma of the tongue is shown.

A, T2-weighted Turbo SE image shows small high-signal intensity mass (*arrowhead*) adjacent to pyriform sinus that was difficult to discern on T1-weighted images. Endoscopic examination of this region was performed twice, yielding no abnormal findings.

B, T2-weighted Turbo spin-echo image (200/105/2/17 [TR/TE/NSA/ETL]) obtained with 59-s scanning time shows needle (*arrow*) with tip positioned within solid anterior portion of lesion. Cytologic analysis revealed squamous cell carcinoma.

Reproduced with permission from reference 27.

FIG 11.   MR-guided sclerotherapy performed in a 31-year-old man with a large, low-flow vascular malformation in the right masticator space. A single frame from a continuous series of FISP images (18/7/1/90°[TR/TE/NSA/flip angle], 1.8-s scanning time) obtained during treatment session shows needle placed from a paramaxillary approach into the deep right masticator space (*arrowheads*). Collection of high signal around needle tip represents a mixture of sclerosing and contrast agents (*arrow*). The needle was repositioned interactively until the entire targeted portion was injected. Follow-up images revealed thrombosis and fibrosis of the malformation, and symptoms of bleeding on dental manipulation and inability to open mouth completely resolved after treatment.

the chosen approach (22, 56). Of particular interest has been use of the tissue discrimination provided by intraoperative MR images to direct the surgeon to areas of residual tumor that may not be apparent by visual inspection. This failure of direct or microscope-assisted vision is usually caused by interposed normal tissue blocking the surgeon's view, or by the similar appearance between primary parenchymal brain tumor and adjacent normal tissue.

Both frame-based and frameless stereotactic systems for neurosurgical guidance provide an alternative for several of these applications. Stereotactic
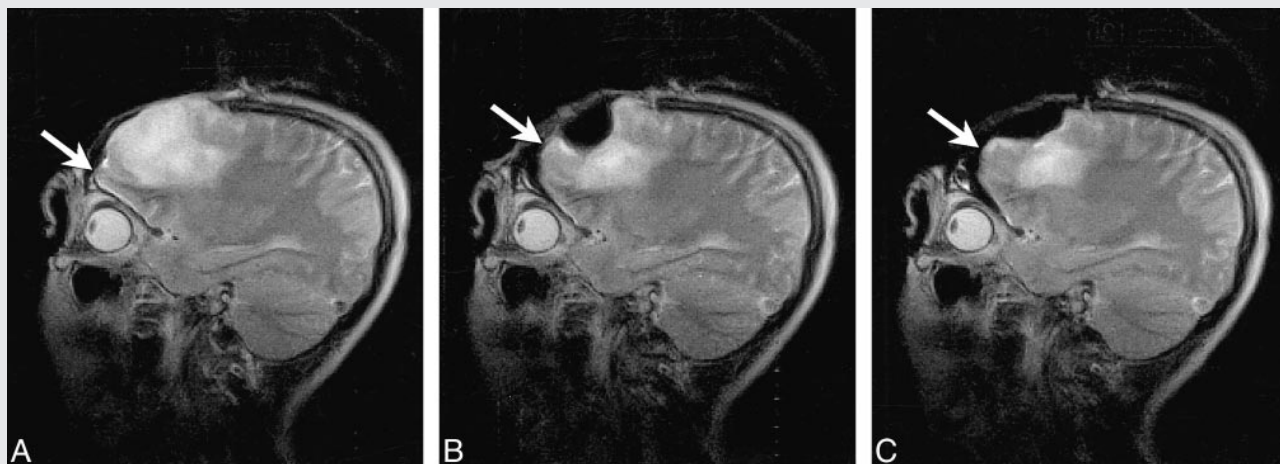
Fig 12. Intraoperative images obtained during tumor resection in a 32-year-old woman are shown. Turbo SE T2-weighted images (2845/102/2 [TR/TE/NSA]; 3-min, 20-s scanning time) were obtained intermittently to monitor resection of a nonenhancing glioma.

A, Frontal pole is immediately adjacent to the dura prior to resection but after craniotomy and dural incision (*arrow*).

B, During tumor removal, the frontal pole and adjacent tissues shift posteriorly, creating an approximate 5-mm gap between the inner surface of the dura and the adjacent cortex (*arrow*).

C, At a later stage during the debulking process, there is further frontal-pole shift (*arrow*) as intracranial volume decreases with tumor resection. Resection was continued after obtaining this image (not shown). All images were obtained on the 0.2 T surgical suite-based C-arm system depicted in figure 3.

navigation has seen a rapid increase in use over the past 5 years, and has allowed a marked reduction in the surgical invasiveness required for biopsy and resection since its introduction (60). Unfortunately these methods, based on preoperative MR or CT data sets, decrease in accuracy as surgical intervention proceeds and anatomy shifts and is altered as a result of tumor resection (Fig 12) (22). In fact, the loss of accuracy during craniotomy begins prior to actual tumor resection, resulting from fluid shifts, changes in arterial pCO_2, and CSF leakage after opening of the dura (60). Intraoperative brain surface deformation greater than 10 mm has been documented within 1 hour of opening the dura, prior to actual tumor resection, (60) in over half of the patients studied. The error induced by this type of shift may be even larger in the presence of hydrocephalus or preexisting loss of parenchymal volume (22). Owing to these sources of error, the usefulness of stereotactic surgical navigation quickly diminishes during the surgical procedure, and this equipment is often relegated to a remote corner of the surgical suite by the late phases of tumor resection.

As compared to methods based on previously acquired data, intraoperative MR imaging allows localization of a lesion in 3D space, and then permits repeated updates of the localization as tumor is resected and shifts in the tissue and fluid compartments of the brain occur. This updated guidance ability is most important for localization of small lesions, for which the error of previously acquired data-based methods might be unacceptable. More importantly, methods based on preoperative data cannot verify that tumor resection is complete nor guide the surgeon to foci of residual tumor or intraoperative hematomas or other complications of surgery. These latter applications have fueled much of the enthusiasm for intraoperative MR imaging

in the neurosurgical community (22, 56–58). Many of these same concepts can be applied to ENT intervention, in which intraoperative MR imaging has been used to guide endoscopic procedures. Use of MR imaging to guide endoscopic procedures provides an interactive and updated ''road map'' to supplement the limited field of view inherent in the endoscopic sinus surgical technique (61). Intraoperative MR imaging has also been used in conjunction with otolaryngology at our institution to monitor success of treatment for skull base surgery (Fig 13). As intraoperative MR methods improve and mature, it is likely that the number of procedures of interest to the neuroradiology community will continue to grow.

The technical requirements for intraoperative MR imaging are slightly different than those necessary for minimally invasive percutaneous procedures, and include an increased need for sufficient signal-to-noise ratios and spatial resolution in order to allow accurate identification of residual tumor or hemorrhage in addition to patient access during the procedure. Many MR image-guided surgical interventions have been performed at mid- or high-field (3, 22). Although field strength has a large impact on the signal-to-noise ratio, many other factors can be used to compensate for the lower field of resistive or permanent magnet systems, including quadrature coil design, pulse sequence design, image bandwidth, and imager receiver chain circuitry. Our experience, and that of Steinmeier and colleagues (57), suggests that the signal-to-noise ratio and spatial resolution possible at 0.2 T can be sufficient for MR image-guided pituitary surgery. These parameters can accurately delineate macro- and microadenomas during surgery, and reveal and delineate residual tumor, cavernous sinus extension, and hemorrhage (Fig 14) (58, 59). Our experience suggests that 0.2-T systems can also provide suf-
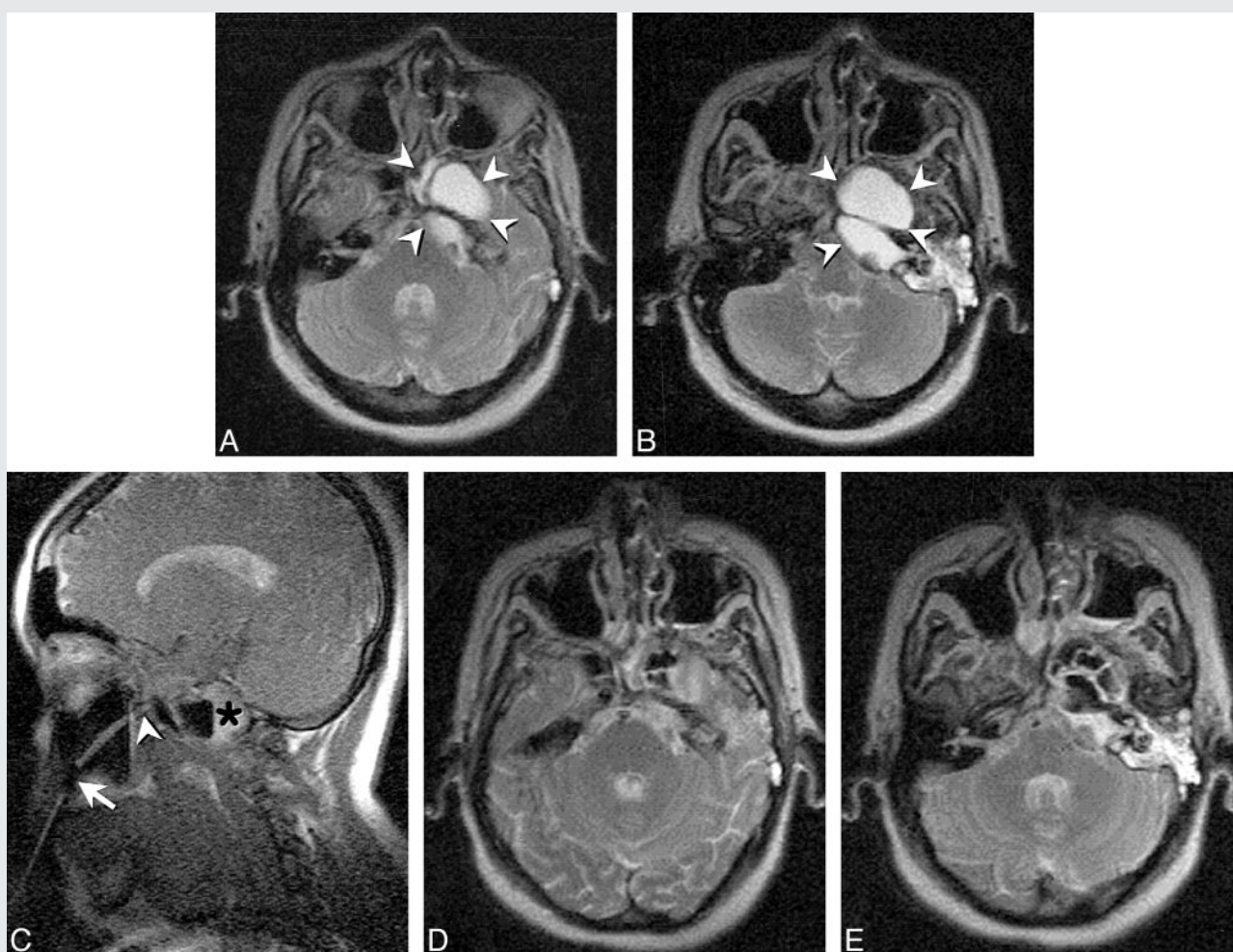
FIG 13.   Imaging of a 49-year-old woman with recurrent skull-base cyst after prior transmaxillary drainage is shown.

A and *B,* Turbo SE T2-weighted axial images (4083/105/5/17 [TR/TE/NSA/ETL], 3-min, 29-s scanning time) show large, multiloculated cyst replacing the petrous apex and body and pterygoid process of the sphenoid bone on the left (*arrowheads*). The bony Eustachian tube is obstructed with a secondary mastoid effusion.

C, FISP image (17.8/8.1/4/90° [TR/TE/NSA/flip angle], 9 s/image) obtained during drainage procedure shows gadolinium-filled catheter extending through Caldwell Luc incision (*arrow*), and pterygopalatine fossa resection site (*arrowhead*) into skull base cyst. Several of the loculations within the cyst are already drained, with residual fluid layering posteriorly (*asterisk*). This frame was one of a continuous series of images obtained during this portion of the procedure.

D and *E,* Turbo SE T2-weighted images, with same parameters as *A* and *B,* show air filling the multiple loculations of the lesion, with a small posterior air-fluid level within the petrous apex portion of the abnormality. Mastoid fluid remains unchanged. Biopsy of cyst wall again revealed normal respiratory epithelium.

ficient image quality to guide the surgeon during craniotomy for tumor resection (Figs 12, 15). The low-field system's capacity to provide this type of guidance has also been established by several other groups. These include researchers from Long Beach Memorial Hospital in California, the University of Cincinnati, the University Hospital in Erlangen, Germany, and, most prominently, the University of Heidelberg where the largest published number of intraoperatively MR-imaged craniotomies (at 0.2 T) have been performed (56, 62, 63). Nonetheless, intraoperative imaging at lower field requires increased imaging time to achieve sufficient image quality for surgical decisions, and the trade-off between imaging time, system cost, and patient access is a matter of ongoing debate.

As with any new technology, it is essential that the initial rush of enthusiasm be followed by care-ful examination to ensure appropriate utilization. It is obvious that many surgical procedures do not require image guidance. Most brain tumors, aneurysms, vascular malformations, and other indications for neurosurgery are performed safely and appropriately with current surgical techniques, including microsurgical methods and both frameless and frame-based stereotaxy. Conversely, certain tumor resections, stereotactic biopsies, thermal ablation of brain tumors, thermal pallidotomy, and functional stimulation procedures lend themselves to the type of sophisticated information provided with intraoperative MR imaging techniques. In particular, the use of intraoperative MR imaging to guide resection of high-grade gliomas, currently being investigated at several centers, must be carefully evaluated prior to widespread adoption in view of the lack of evidence that more complete
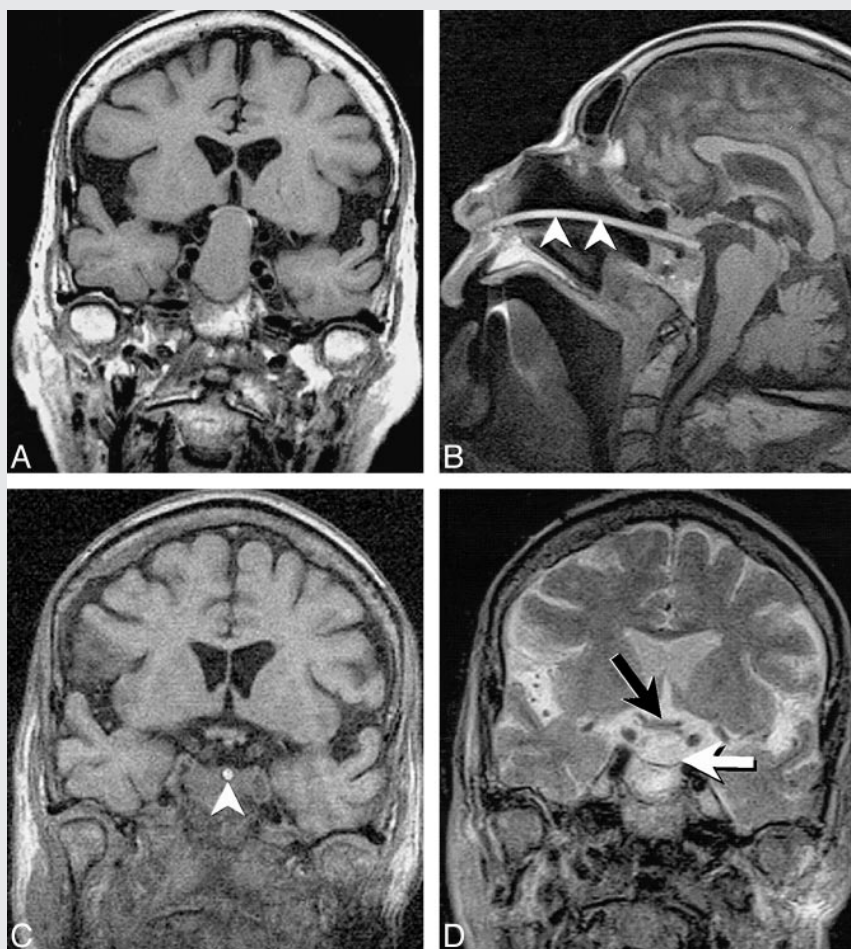
Fig 14. Imaging of a 76 year-old woman with pituitary macroadenoma resulting in visual symptoms is shown.

A, Preoperative coronal T1-weighted (680/14/3) image depicts large macroadenoma resulting in marked elevation and compression of the optic chiasm.

B, Intraoperative sagittal T1-weighted SE image (432/26/3 [TR/TE/NSA], 202 × 256 matrix, 20-cm FOV) shows localizer probe, which can be seen as a bright line (*arrowheads*) extending through the nasal cavity into the sella extending to the posterior aspect of the resection bed.

C, Intraoperative coronal 3D T1-weighted FLASH image (120/12/1/60° [TR/TE/NSA/flip angle], 256 × 256 matrix, 20-cm FOV, 8-min, 15-s scanning time) shows complete decompression of the optic chiasm with a CSF-filled suprasellar cistern. The localizer probe can be seen as a bright circle within the sella (*arrowhead*). Blood and secretions pooling within the sella make it difficult to detect residual tumor on unenhanced T1-weighted images.

D, Coronal turbo SE T2-weighted image (3500/102/1/7 [TR/TE/NSA/ETL], 210 × 256 matrix, 20-cm FOV, 5-min, 2-s scanning time) obtained later in the procedure again reveals decompression of the optic chiasm (*black arrow*) and relaxation of the diaphragma sellae (*white arrow*). On T2-weighted images, fluid or blood pooling within the sella can more easily be distinguished from residual tumor. Contrast-enhanced images are of less help than might be predicted owing to pooling of contrast-enhanced blood within the sella if any oozing occurs before or during image acquisition.

Reproduced with permission from reference 58.

resection increases survival. Although preliminary data suggest that MR guidance may decrease the size of craniotomy and therefore shorten hospital stay (22), careful cost analysis is necessary to document any advantages from the addition of intraoperative imaging to the surgical procedure.

Economic Considerations

In addition to the many engineering challenges related to MR procedural guidance, the development of appropriate guidelines to optimize cost-effectiveness of these interventions also represents a difficult task. When compared to current sonography-and CT-guided procedures, MR-guided procedures are slightly more expensive (charges for an MR-guided procedure are currently approximately 10% to 15% more than for a similar procedure under CT guidance at our institution). Therefore, when less expensive CT or sonographic guidance is suitable, their use is warranted as the most cost-effective choice. There are a number of procedures in which other imaging techniques lack the tissue contrast or vascular conspicuity to provide safe routes for biopsy or aspiration (27). It is these procedures, for which other imaging applications are limited or open surgical biopsy is the primary alternative, that provide the best indication for MR-guided techniques.

Many of the most formidable barriers to widespread dissemination of these techniques have been the economic issues related to interventional MR imaging. Often obtaining the necessary financial resources for acquiring interventional MR imaging capabilities can be considered an insurmountable problem outside of the academic setting. The cost and setup of an interventional system depends on several factors, including field strength and system fringe field, and the more novel the interventional design, the more expensive its acquisition. The least expensive approach for percutaneous procedures is to add the necessary supplemental equipment for MR image-guided procedures to an existing diagnostic MR system. Several vendors offer interventional accessories below $160,000, making the variable cost required to perform percutaneous MR-guided procedures relatively low for those sites with preexisting open MR scanners. Purchase and setup of a low-field system specifically outfitted for intervention, such as a 1.5-T superconducting short-bore or ''double-donut'' system, become progressively more expensive. As the speed at which these procedures can be performed further increases with improvements in MR guidance tech-
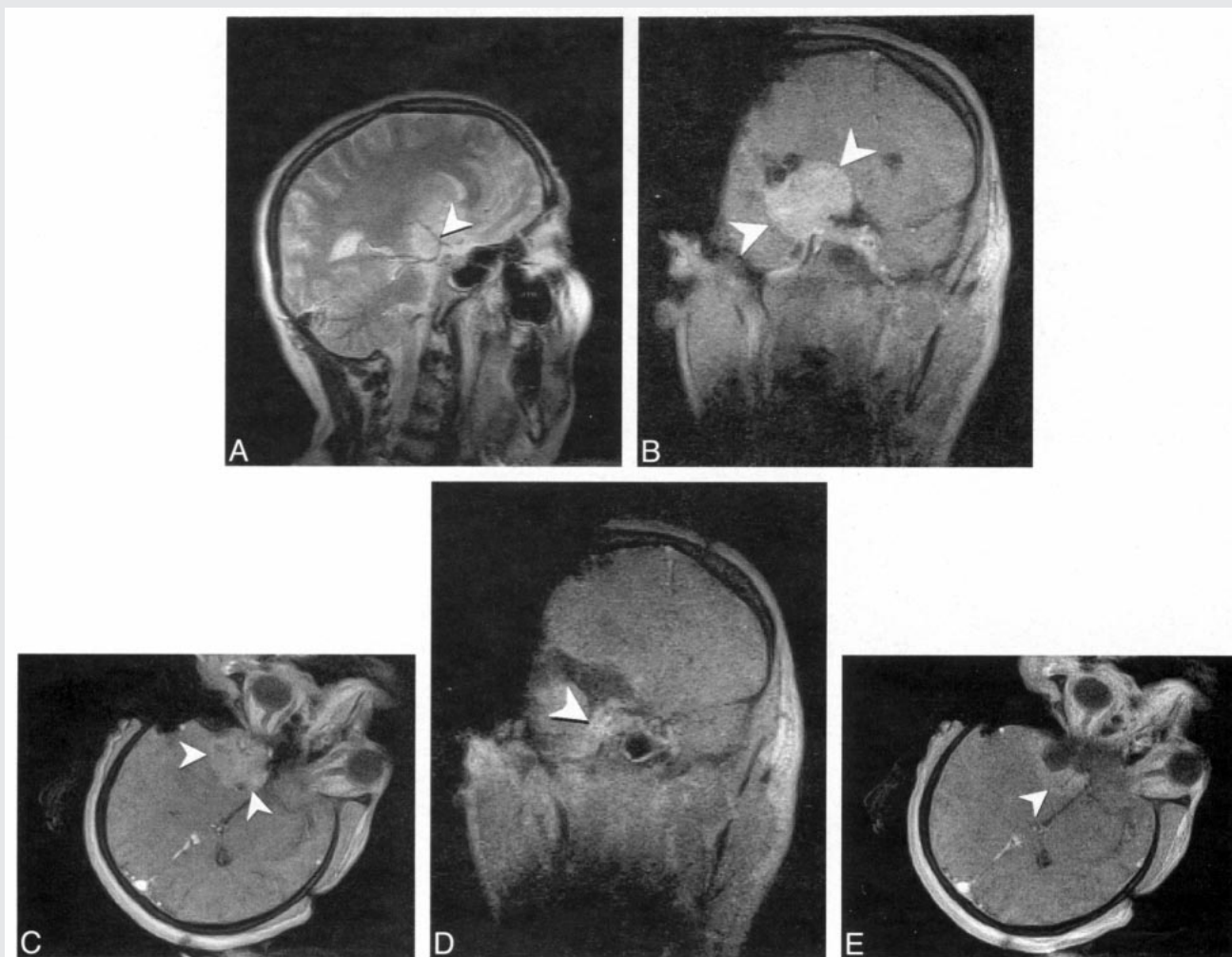
FIG 15.   Imaging of a 40-year-old woman with sphenoid wing meningioma is shown.
   A, Intraoperative turbo SE T2-weighted oblique image (2598/105/5/17 [TR/TE/NSA/ETL], 2-min, 40-s scanning time) reveals sphenoid wing mass encasing the bifurcation of the middle cerebral artery (MCA) (*arrowhead*).
   B and *C,* Coronal (*B*) and axial (*C*) contrast-enhanced FLASH T1-weighted images (110/9/5/70° [TR/TE/NSA/flip angle], 1-min, 48-s scanning time) reveals meningioma after craniotomy and surgical exposure. The margins of the lesion and location of the optic chiasm, ICA, and primary MCA branches were determined interactively using gadolinium-filled markers.
   D and *E,* Coronal (*D*) and axial (*E*) images obtained after resection, with same parameters as *A,* show gross debulking of the tumor with a thin rim of enhancing tissue intentionally left along the cavernous sinus and encased arteries (*arrowheads*).

niques, the contribution to fixed cost as compared to CT guidance should continue to decrease.

Finally, even with the current level of technology and expense, appropriate use of interventional MR imaging can result in a tremendous potential reduction in the costs associated with treating certain patients. In particular, for patients in whom the application of MR image-guided biopsy, thermal ablation, or chemical ablation can help avoid an open surgical procedure, there has been a marked decrease in cost at our institution. This has resulted from decreased procedural cost, relative to surgery, along with equal or more pronounced savings through avoidance of intensive and routine care hospitalization. This is in addition to the patient's benefit that results from reduced morbidity, mortality, postprocedural discomfort, and recovery time when open surgical procedures can be avoided. These potential advantages of interventional MR imaging have provided the rationale for an in-

creased interest in these techniques, with a growing number of centers and radiology practices developing interventional or intraoperative MR imaging capabilities. The overall success for this developing field within interventional radiology will require the careful application of these techniques to ensure appropriate use. Intraoperative and minimally invasive MR-guided techniques hold tremendous potential, but much effort remains necessary to define their appropriate role in the delivery of cost-effective medical care.

Acknowledgments

References

1. Kahn T, Harth T, Bettag M, et al. **Preliminary experience with the application of gadolinium-DTPA before MR imaging-guided laser-induced interstitial thermotherapy of brain tumors.** *J Magn Reson Imaging* 1997;7:226–229

2. Vogl TJ, Mack MG, Muller P, et al. **Recurrent nasopharyngeal tumors: preliminary clinical results with interventional MR imaging–controlled laser-induced thermotherapy.** *Radiology* 1995;196:725–733

3. Liu H, Martin AJ, Truwit CL. **Interventional MRI at high-field (1.5 T): needle artifacts.** *J Magn Reson Imaging* 1998;8:214–219

4. Hinks RS, Bronskill MJ, Kucharczyk W, Bernstein M, Collick BD, Henkelman RM. **MR systems for image-guided therapy.** *JMRI* 1998;8:19–25

5. Mueller PR, Stark DD, Simeone JF, et al. **MR-guided aspiration biopsy: needle design and clinical trials.** *Radiology* 1986;161:605–609

6. Lufkin R, Teresi L, Hanafee W. **New needle for MR-guided aspiration cytology of the head and neck.** *AJR Am J Roentgenol* 1987;149:380–382

7. Lufkin R, Duckwiler G, Spickler E, Teresi L, Chang M, Onik G. **MR body stereotaxis: an aid for MR-guided biopsies.** *J Comput Assist Tomogr* 1988;12:1088–1089

8. Kaufman L, Arakawa M, Hale J, et al. **Accessible magnetic resonance imaging.** *Magn Reson Q* 1989;5:283–297

9. Gronemeyer DH, Kaufman L, Rothschild P, Seibel RM. **[New possibilities and aspects of low-field magnetic resonance tomography].** *Radiol Diagn (Berl)* 1989;30:519–527

10. Lufkin R, Teresi L, Chiu L, Hanafee W. **A technique for MR-guided needle placement.** *AJR Am J Roentgenol* 1988;151:193–196

11. Duckwiler G, Lufkin RB, Teresi L, et al. **Head and neck lesions: MR-guided aspiration biopsy.** *Radiology* 1989;170:519–522

12. Wenokur R, Andrews JC, Abemayor E, et al. **Magnetic resonance imaging-guided fine needle aspiration for the diagnosis of skull base lesions.** *Skull Base Surg* 1992;2:167–170

13. Castro DJ, Lufkin RB, Saxton RE, et al. **Metastatic head and neck malignancy treated using MRI guided interstitial laser phototherapy: an initial case report.** *Laryngoscope* 1992;102:26–32

14. Kahn T, Bettag M, Ulrich F et al. **MRI-guided laser-induced interstitial thermotherapy of cerebral neoplasms.** *J Comput Assist Tomogr* 1994;18:519–532

15. Anzai Y, Lufkin R, DeSalles A, Hamilton DR, Farahani K, Black KL. **Preliminary experience with MR-guided thermal ablation of brain tumors.** *AJNR Am J Neuroradiol* 1995;16:39–48

16. Jager L, Muller-Lisse GU, Gutmann R, Feyh J, Thoma M, Reiser M. **[Initial results with MRI-controlled laser-induced interstitial thermotherapy of head and neck tumors].** *Radiologe.* 1996;36:236–244

17. Strother CM, Unal O, Frayne R, Korosec FR, Mistretta CA. **Feasibility study of the endovascular treatment of experimental canine aneurysms using MR guidance [abstract].** *Radiology* 1998;319:–209P[S]

18. Orel SG, Schnall MD, Newman RW, Powell CM, Torosian MH, Rosato EF. **MR imaging-guided localization and biopsy of breast lesions: initial experience.** *Radiology* 1994;193:97–102

19. Schenck JF, Jolesz FA, Roemer PB, et al. **Superconducting open-configuration MR imaging system for image-guided therapy.** *Radiology* 1995;195:805–814

20. Silverman SG, Collick BD, Figueira MR, et al. **Interactive MR-guided biopsy in an open-configuration MR imaging system.** *Radiology* 1995;197:175–181

21. Silverman SG, Jolesz FA, Newman RW, et al. **Design and implementation of an interventional MR imaging suite.** *AJR Am J Roentgenol* 1997;168:1465–1471

22. Black PM, Moriarty T, Alexander E, et al. **Development and implementation of intraoperative magnetic resonance imaging and its neurosurgical applications.** *Neurosurgery* 1997;41:831–842

23. Alexander E, Moriarty TM, Kikinis R, Black P, Jolesz FM. **The present and future role of intraoperative MRI in neurosurgical procedures.** *Stereotact Funct Neurosurg* 1997;68:10–17

24. Saunders JK, Hoult D, Sutherland G. **The swinging magnet: an MRI adjunct to neurosurgery.** Paper presented at: Annual Meeting of the International Society for Magnetic Resonance in Medicine. April 1997; Vancouver, B.C.

25. Mahfouz AE, Rahmouni A, Zylbersztejn C, Mathieu D. **MR-guided biopsy using ultrafast T1- and T2- weighted reordered turbo fast low-angle shot sequences: feasibility and preliminary clinical applications.** *AJR Am J Roentgenol* 1996;167:167–169

26. Duerk JL, Lewin JS, Wendt M, Petersilge C. **Remember true FISP? A high SNR, near 1-second imaging method for T2-like contrast in interventional MRI at .2 T.** *J Magn Reson Imaging* 1998;8:203–208

27. Lewin JS, Petersilge CA, Hatem SF, et al. **Interactive MR imaging-guided biopsy and aspiration with a modified clinical C-arm system.** *AJR Am J Roentgenol* 1998;170:1593–1601

28. Chung YC, Merkle EM, Lewin JS, Shonk JR, Duerk JL. **Fast T2-weighted imaging by PSIF at 0.2T for interventional MR.** *Magn Reson Med.* In press.

29. Busch M, Bornstedt A, Wendt M, Duerk JL, Lewin JS, Groenemeyer D. **Fast "real time" imaging with different k-space update strategies for interventional procedures.** *J Magn Reson Imaging* 1998;8:944–954

30. Duerk JL, Lewin JS, Wu DH. **Application of keyhole imaging to interventional MRI: a simulation study to predict sequence requirements.** *J Magn Reson Imaging* 1996;6:918–924

31. Panych LP, Oesterle C, Zientara GP, Hennig J. **Implementation of a fast gradient-echo SVD encoding technique for dynamic imaging.** *Magn Reson Med* 1996;35:554–562

32. Cao Y, Levin DN. **On the relationship between feature-recognizing MRI and MRI encoded by singular value decomposition.** *Magn Reson Med* 1995;33:140–142

33. Duerk JL, Wu DH, Chung YC, Liang ZP, Lewin JS. **A simulation study to assess SVD encoding for interventional MRI: effect of object rotation and needle insertion.** *J magn Reson Imaging* 1996;6:957–960

34. Zientara GP, Panych LP, Jolesz FA. **Dynamically adaptive MRI with encoding by singular value decomposition.** *Magn Reson Med* 1994;32:268–274

35. Gelman N, Wood ML. **Wavelet encoding for improved SNR and retrospective slice thickness adjustment.** *Magn Reson Med.* 1998;39:383–391

36. Panych LP, Jakab PD, Jolesz FA. **Implementation of wavelet-encoded MR imaging.** *J Magn Reson Imaging* 1993;3:649–655

37. Panych LP, Jolesz FA. **A dynamically adaptive imaging algorithm for wavelet-encoded MRI.** *Magn Reson Med.* 1994;32:738–748

38. Panych LP, Mulkern RV, Saiviroonporn P, Zientara GP, Jolesz FA. **Non-Fourier encoding with multiple spin echoes.** *Magn.Reson Med* 1997;38:964–973

39. Peters RD, Wood ML. **Multilevel wavelet-transform encoding in MRI.** *J Magn Reson Imaging* 1996;6:529–540

40. Weaver JB, Xu Y, Healy DM, Driscoll JR. **Wavelet-encoded MR imaging.** *Magn Reson Med* 1992;24:275–287

41. Wendt M, Busch M, Lenz G, et al. **Dynamic Tracking Algorithm for Interventional MRI using Wavelet-Encoding in Gradient-Echo Sequences.** *IEE Trans Med Imaging* 1998;17:803–809

42. Lewin JS, Duerk JL, Jain VR, Petersilge CA, Chao CP, Haaga JR. **Needle localization in MR-guided biopsy and aspiration: effects of field strength, sequence design, and magnetic field orientation.** *AJR Am J Roentgenol* 1996;166:1337–1345

43. Frahm C, Gehl HB, Melchert UH, Weiss HD. **Visualization of magnetic resonance-compatible needles at 1.5 and 0.2 Tesla.** *Cardiovasc Intervent Radiol* 1996;19:335–340

44. Gehl HB, Frahm C, Schimmelpenning H, Weiss HD. **[A technique of MRT-guided abdominal drainage with an open low-field magnet. Its feasibility and the initial results.]** *Rofo Fortschr Geb Rontgenstr Neuen Bildgeb Verfahr* 1996;165:70–73

45. Hathout G, Lufkin RB, Jabour B, Andrews J, Castro D. **MR-guided aspiration cytology in the head and neck at high field strength.** *J Magn Reson Imaging* 1992;2:93–94

46. Vogl TJ, Mack MG, Straub R, Roggan A, Felix R. **Percutaneous MRI-guided laser-induced thermotherapy for hepatic metastases for colorectal cancer.** *Lancet* 1997;350:29–29

47. Lewin JS, Connell CF, Duerk JL, et al. **Interactive MRI-guided radiofrequency interstitial thermal ablation of abdominal tumors: clinical trial for evaluation of safety and feasibility.** *J Magn Reson Imaging* 1998;8:40–47

48. Jolesz FA, Bleier AR, Jakab P, Ruenzel PW, Huttl K, Jako GJ. **MR imaging of laser-tissue interactions.** *Radiology* 1988;168:249–253

49. Harth T, Kahn T, Rassek M, et al. **Determination of laser-induced temperature distributions using echo-shifted Turbo-FLASH.** *Magn Reson Med* 1997;38:238–245

50. Chung YC, Duerk JL, Shankaranarayanan A, Hampke M, Merkle EM, Lewin JS. **Temperature Measurement Using Echo-Shifted Flash at Low Field for Interventional MRI.** *J Magn Reson Imaging* 1999;9:138–145
51. Farahani K, Mischel PS, Black KL, De SA, Anzai Y, Lufkin RB. **Hyperacute thermal lesions: MR imaging evaluation of development in the brain.** *Radiology* 1995;196:517–520
52. Boaz TL, Lewin JS, Chung YC, Duerk JL, Clampitt ME, Haaga JR. **MR monitoring of MR-guided radiofrequency thermal ablation of normal liver in an animal model.** *J Magn Reson Imaging* 1998;8:64–69
53. Kahn T, Harth T, Kiwit JC, Schwarzmaier HJ, Wald C, Modder U. **In vivo MRI thermometry using a phase-sensitive sequence: preliminary experience during MRI-guided laser-induced interstitial thermotherapy of brain tumors.** *J Magn Reson Imaging* 1998;8:160–164
54. Schwabe B, Kahn T, Harth T, Ulrich F, Schwarzmaier HJ. **Laser-induced thermal lesions in the human brain: short- and long-term appearance on MRI.** *Jcomput Assist Tomogr* 1997;21: 818–825
55. Lewin JS, Merkle E, Duerk JL, Tarr R. **MR image-guided percutaneous sclerotherapy of low-flow vascular malformations in the head and neck: safety and feasibility-preliminary experience with 14 procedures in 3 patients.** *Radiology* 1999;211:566–570
56. Tronnier VM, Wirtz CR, Knauth M, et al. **Intraoperative diagnostic and interventional magnetic resonance imaging in neurosurgery.** *Neurosurgery* 1997;40:891–900
57. Steinmeier R, Fahlbusch R, Ganslandt O, et al. **Intraoperative magnetic resonance imaging with the magnetom open scanner: concepts, neurosurgical indications, and procedures: a preliminary report.** *Neurosurgery* 1998;43:739–747
58. Hlavin ML, Lewin JS, Arafah BM, Cesar A, Clampitt ME, Selman WR. **Intraoperative magnetic resonance imaging for assessment of chiasmatic decompression and tumor resection during transsphenoidal pituitary surgery.** *Techniques in Neurosurgery* In press.
59. Lewin JS, Hlavin ML, Duerk JL, Clampitt ME, Selman WR. **Intra-operative MR imaging for guidance of trans-sphenoidal procedures: imaging characteristics and issues.** Presented at: the Annual Meeting International Society for Magnetic Resonance in Medicine. 1998; Sydney, Australia.
60. Hill DL, Maurer CRJ, Maciunas RJ, Barwise JA, Fitzpatrick JM, Wang MY. **Measurement of intraoperative brain surface deformation under a craniotomy.** *Neurosurgery* 1998;43:514–526
61. Fried MP, Topulos G, Hsu L, et al. **Endoscopic sinus surgery with magnetic resonance imaging guidance: initial patient experience.** *OtolaryngolHead.Neck Surg* 1998;119:374–380
62. Wirtz CR, Tronnier VM, Bonsanto MM, et al. **Image-guided neurosurgery with intraoperative MRI: update of frameless stereotaxy and radicality control.** *Stereotact Funct Neurosurg* 1997; 68:39–43
63. Knauth M, Wirtz CR, Tronnier VM, Staubert A, Kunze S, Sartor K. **[Intraoperative magnetic resonance tomography for control of extent of neurosurgical operations].** *Radiologe* 1998; 38:218–224